

# Personalized Chronomodulated 5-Fluorouracil Treatment: A Physiologically-Based Pharmacokinetic Precision Dosing Approach for Optimizing Cancer Therapy

Fatima Zahra Marok<sup>1</sup>, Jan-Georg Wojtyniak<sup>1,2</sup> , Dominik Selzer<sup>1</sup> , Robert Dallmann<sup>3</sup>, Jesse J. Swen<sup>4</sup> , Henk-Jan Guchelaar<sup>4</sup> , Matthias Schwab<sup>2,5,6</sup>  and Thorsten Lehr<sup>1,\*</sup> 

The discovery of circadian clock genes greatly amplified the study of diurnal variations impacting cancer therapy, transforming it into a rapidly growing field of research. Especially, use of chronomodulated treatment with 5-fluorouracil (5-FU) has gained significance. Studies indicate high interindividual variability (IIV) in diurnal variations in dihydropyrimidine dehydrogenase (DPD) activity – a key enzyme for 5-FU metabolism. However, the influence of individual DPD chronotypes on chronomodulated therapy remains unclear and warrants further investigation. To optimize precision dosing of chronomodulated 5-FU, this study aims to: (i) build physiologically-based pharmacokinetic (PBPK) models for 5-FU, uracil, and their metabolites, (ii) assess the impact of diurnal variation on DPD activity, (iii) estimate individual DPD chronotypes, and (iv) personalize chronomodulated 5-FU infusion rates based on a patient's DPD chronotype. Whole-body PBPK models were developed with PK-Sim<sup>(R)</sup> and MoBi<sup>(R)</sup>. Sinusoidal functions were used to incorporate variations in enzyme activity and chronomodulated infusion rates as well as to estimate individual DPD chronotypes from *DPYD* mRNA expression or DPD enzymatic activity. Four whole-body PBPK models for 5-FU, uracil, and their metabolites were established utilizing data from 41 5-FU and 10 publicly available uracil studies. IIV in DPD chronotypes was assessed and personalized chronomodulated administrations were developed to achieve (i) comparable 5-FU peak plasma concentrations, (ii) comparable 5-FU exposure, and (iii) constant 5-FU plasma levels via “noise cancellation” chronomodulated infusion. The developed PBPK models capture the extent of diurnal variations in DPD activity and can help investigate individualized chronomodulated 5-FU therapy through testing alternative personalized dosing strategies.

## Study Highlights

### WHAT IS THE CURRENT KNOWLEDGE ON THE TOPIC?

✓ 5-Fluorouracil (5-FU) is a widely used anticancer drug, that is influenced by diurnal variations and often administered as chronomodulated intravenous infusions. Pronounced interindividual variability (IIV) of dihydropyrimidine dehydrogenase (DPD) chronotypes was shown in patients with cancer.

### WHAT QUESTION DID THIS STUDY ADDRESS?

✓ The presented study aimed to question the use of uniformed chronomodulated 5-FU treatment on an individual patient level.

### WHAT DOES THIS STUDY ADD TO OUR KNOWLEDGE?

✓ Physiologically-based pharmacokinetic (PBPK) models of endogenous uracil and 5-FU together with their respective

metabolites formed by DPD were developed to include the impact of diurnal variations on DPD and to investigate the influence of IIV in DPD chronotypes for 5-FU exposure during various treatment scenarios.

### HOW MIGHT THIS CHANGE CLINICAL PHARMACOLOGY OR TRANSLATIONAL SCIENCE?

✓ With help of the successfully developed PBPK models, the study proposes a new and personalized treatment approach of 5-FU therapy based on an individuals' DPD chronotype.

<sup>1</sup>Clinical Pharmacy, Saarland University, Saarbruecken, Germany; <sup>2</sup>Dr. Margarete Fischer-Bosch-Institut of Clinical Pharmacology, Stuttgart, Germany; <sup>3</sup>Division of Biomedical Sciences, Warwick Medical School, University of Warwick, Coventry, UK; <sup>4</sup>Department of Clinical Pharmacy & Toxicology, Leiden University Medical Center, RC Leiden, The Netherlands; <sup>5</sup>Departments of Clinical Pharmacology, and of Biochemistry and Pharmacy, University Tuebingen, Tuebingen, Germany; <sup>6</sup>Cluster of excellence iFIT (EXC2180) “Image-Guided and Functionally Instructed Tumor Therapies”, University Tuebingen, Tuebingen, Germany. \*Correspondence: Thorsten Lehr ([thorsten.lehr@mx.uni-saarland.de](mailto:thorsten.lehr@mx.uni-saarland.de))

Received August 4, 2023; accepted January 3, 2024. doi:10.1002/cpt.3181

5-Fluorouracil (5-FU) is a potent anticancer agent that is extensively used in treatment of various cancers, for example, as first-line treatment in combinations with other anticancer drugs.<sup>1,2</sup> Given its structural similarity to the endogenous nucleobase uracil, 5-FU effectively inhibits tumor growth by interfering with the synthesis of DNA, RNA, and other nucleosides. Due to its highly variable oral bioavailability (ranging from 0 to 80%), narrow therapeutic window,<sup>2</sup> and improved toxicity profile, 5-FU is commonly administered as a combination of an intravenous bolus injection followed by a continuous infusion, or solely as a continuous infusion over a period of 22–96 hours, in repeated cycles covering several months of treatment.<sup>3</sup>

Dihydropyrimidine dehydrogenase (DPD) catalyzes the rate-limiting reaction in the conversion of 5-FU to inactive metabolites. Several genetic variants within the gene coding for DPD (*DPYD*) have been identified that lead to altered enzyme activity and subsequently result in reduced 5-FU metabolism.<sup>4</sup> Thus, considering the narrow therapeutic window,<sup>2</sup> certain *DPYD* alleles are associated with potentially life-threatening toxicities during chemotherapy.<sup>1,4,5</sup> Furthermore, cellular circadian clocks strongly modulate 5-FU metabolic pathways, which can affect both catabolic pathways, such as DPD metabolism, as well as anabolic pathways, for example, mediated by the uridine monophosphate synthase. Specifically, diurnal variation significantly influences the expression of *DPYD* messenger RNA (mRNA) and, hence, DPD biosynthesis. This leads to pronounced diurnal patterns in plasma levels of its endogenous substrate uracil, as well as the ratio of dihydrouracil-to-uracil (DHU/U).<sup>6–9</sup> Additionally, studies have indicated diurnal variations in plasma concentrations of 5-FU during continuous constant-rate infusions, as reported in the literature.<sup>10–13</sup> Notably, these studies have documented inter- and intraindividual variability regarding both the time and extent of peak DPD activity.<sup>8,14,15</sup> Chronomodulated 5-FU treatment schedules have peak infusion rates at 4AM,<sup>6</sup> often in various combinations with chronomodulated irinotecan and oxaliplatin like the chronoFLO4 treatment.<sup>6,16,17</sup> Compared with constant-rate infusions, chronomodulated infusions with peak delivery at 4AM were better tolerated by male patients, whereas female patients experienced more grade 3–4 toxicities and demonstrated decreased response rates and overall survival under chronomodulated treatment.<sup>16,17</sup> Mathematical analyses using semimechanistic models unveiled considerable interpatient variability in the pharmacokinetics (PK) during chronomodulated therapy with 5-FU.<sup>18</sup> Despite all patients receiving 5-FU treatment (combined with irinotecan and oxaliplatin) with the same peak delivery rate and relative dose per body surface area, significant differences in maximum plasma concentrations ( $C_{max}$ ) and areas under plasma concentration-time curves (AUC) could be observed.<sup>18,19</sup> As 5-FU clearance strongly correlates with DPD activity, interindividual variability (IIV) regarding diurnal DPD-mediated 5-FU metabolism could attribute significantly to the variability observed in 5-FU plasma exposure.<sup>20</sup>

In order to better understand the intricate interplay between the circadian clock and the time-of-day dependent variation in

5-FU therapy, our primary objective in this study was to formulate a personalized strategy for chronomodulated 5-FU treatment. We achieved this by using physiologically-based pharmacokinetic (PBPK) modeling, a mathematical technique to describe and predict a drug's behavior in various physiological tissues. Here, the versatility of the whole-body PBPK framework enables the exploration of various treatment scenarios, including intravenous, intra-arterial, or oral administrations of 5-FU.

Thus, the objectives of this study are as follows: (i) to predict the impact of diurnal variation on time-dependent DPD-mediated metabolism by developing whole-body PBPK models for 5-FU, uracil, and their metabolites dihydrofluorouracil (DHFU) and dihydrouracil (DHU); (ii) to simulate continuous infusions of 5-FU with chronomodulated administration rates; (iii) to estimate individual DPD chronotypes based on observed mRNA expressions, enzyme activities, or endogenous uracil levels; and (iv) to ultimately derive personalized chronomodulated 5-FU treatment tailored to the estimated individual DPD chronotypes.

## METHODS

### Software

For model development, PK-Sim and MoBi (Open Systems Pharmacology Suite 9.1, released under the GPLv2 license by the Open Systems Pharmacology community, [www.open-systems-pharmacology.org](http://www.open-systems-pharmacology.org))<sup>21</sup> were utilized. Model parameter estimation was carried out using Monte Carlo and Levenberg–Marquardt algorithms implemented in PK-Sim<sup>(R)</sup> and MoBi<sup>(R)</sup>. Published concentration-time profiles of 5-FU, uracil, and their metabolites were digitized using GetData Graph Digitizer (version 2.26.0.20, S. Fedorov). PK parameter analysis, model performance evaluation, and figures were generated using the R programming language (version 3.6.3, R Core Team; R: A Language and Environment for Statistical Computing. R Foundation for Statistical Computing, Vienna, Austria, 2021).

### Clinical data

Data from clinical studies of 5-FU and uracil were obtained from the literature and digitized following the approach of Wojtyniak and coworkers.<sup>22</sup> Plasma concentration-time profiles of endogenous uracil, [ $^{13}C$ ] uracil after oral administration in healthy subjects, and 5-FU during and after intravenous administration in patients with cancer were compiled and divided into a training and a test data set used for model building and model evaluation, respectively. The training data set included metabolite concentration-time profiles, a broad dosing range, and various administration protocols. To account for the known sex differences, studies were assigned to the respective training and test data sets for a balanced distribution of female and male subjects. Demographic information of all collected profiles can be found in the clinical study tables in [Sections S2 and S3](#) of the Supplementary Materials.

### PBPK model building

An extensive literature search was conducted to gather data on the physicochemical properties, PK processes, as well as clinical studies. Whole-body PBPK models were built with virtual individuals based on the mean and mode of reported demographic information, including age, body weight, height, ethnicity, and sex for each study. If demographic data were unavailable for a study, virtual standard individuals were created with details listed in [Table S1.3](#). Tissue distributions of relevant enzymes

and transporters were implemented, using the PK-Sim<sup>(R)</sup> expression database.<sup>23</sup> Detailed information on the used expression profiles derived from the PK-Sim<sup>(R)</sup> expression database is provided in **Tables S1.1** and **S1.2**.

Model input parameters that could not be sufficiently informed from the literature or were involved in important quantitative structure–activity relationship model estimates of permeability and distribution processes were optimized by fitting the models simultaneously to all plasma concentration–time profiles of the training data set.

### Implementation of diurnal variations

For simulations of continuous infusions, a time-dependent sine function was used to describe oscillation over 24 hours (Eq. 1) accounting for diurnal variations in enzyme activity of DPD and dihydropyrimidinase (DPH), which catalyzes biotransformations of 5-FU and uracil metabolites. Similarly, variations in chronomodulated infusion rates were also calculated according to (Eq. 1):

$$f(t) = \left( 1 + \text{Amp} * \sin\left(\frac{2\pi(t + T_{\text{Acr}})}{24}\right) \right) * V \quad (1)$$

where Amp is the amplitude,  $t$  represents the simulation time in hours,  $T_{\text{Acr}}$  is the phase shift, and  $V$  is the respective enzymatic activity rate or infusion rate.

The amplitude was either derived from studies reporting mean DPD activities over a period of 24 hours<sup>7,9</sup> for the majority of studies, or adjusted to fit the respective observed plasma concentrations, as listed in **Table S3.3**. Because the time of peak DPD activity (acrophase) and resulting minimal 5-FU plasma concentrations differed between several studies,<sup>15,18,20,24</sup> a mean phase shift parameter  $T_{\text{Acr}}$  could not be derived from the literature. Hence, if no data on DPD activity of patients were available and their respective acrophase was unknown,  $T_{\text{Acr}}$  was estimated. This estimation was also necessary if information regarding the time-of-day for the start of 5-FU administration or plasma concentration measurements was missing. When incorporating diurnal variations in DPH activity, values for Amp and  $T_{\text{Acr}}$  (Eq. 1) were estimated, as no activity profiles were available in the existing literature.

### PBPK model evaluation

Model performance was evaluated by visual predictive checks of predicted and observed profiles from the corresponding clinical studies. Moreover, goodness-of-fit plots of predicted vs. observed plasma concentrations, AUC calculated from the time of the first to the last concentration measurement ( $\text{AUC}_{\text{last}}$ ) as well as  $C_{\text{max}}$  values were generated. To quantify the descriptive and predictive performance of the models, mean relative deviation (MRD) and median symmetric accuracy (MSA) of all plasma concentration predictions together with geometric mean fold error (GMFE) of all AUC and  $C_{\text{max}}$  predictions were computed. For this, MRD and GMFE values  $\leq 2$  were considered successful model predictions. Details on the quantitative model evaluation can be found in **Section S1.1**.

Local sensitivity to single parameter changes was analyzed for the AUC of 5-FU, uracil, and their metabolites as described in **Section S1.2** with visualized results in **Section S2.4.5** and **S3.4.5**.

### In vitro–in vivo-extrapolation of individual DPD chronotypes for dose individualizations

To estimate individual DPD chronotypes, diurnal patterns were derived from *in vitro* measurements of DPD activities or from *in vitro* measurements of *DPYD* mRNA expressions, which were then translated into DPD activities.<sup>7,8</sup> Next, the Amp and  $T_{\text{Acr}}$  of the diurnal pattern (see Eq. 1) were estimated to fit the observed DPD activities. Subsequently, the estimated diurnal parameters served as input for the DPD-mediated biotransformation in *in vivo* predictions of 5-FU or uracil plasma concentrations with the developed PBPK models.

## RESULTS

### PBPK model development: Implementation of diurnal variations

Whole-body PBPK models for 5-FU, uracil, and their metabolites DHFU and DHU were developed based on clinical data from 41 5-FU studies involving 777 patients and 10 uracil studies involving 104 volunteers. The administered doses of 5-FU ranged from 140 to 600 mg/m<sup>2</sup> for injections, 250–1750 mg/m<sup>2</sup>/day for infusions and 300–580 mg/m<sup>2</sup> for oral solutions. Oral [2-<sup>13</sup>C]uracil studies involved dosing ranging from 50 to 1,000 mg. Overall, 16 profiles were compiled in the training data set and 89 profiles were used for the test data set. All clinical studies used for model development are listed in **Tables S2.1**, **S3.1**, and **S4.1**.

A structure of the whole-body 5-FU and uracil PBPK models is depicted in **Figure 1a**. The biotransformation of 5-FU and uracil via DPD to DHFU and DHU, respectively, which are then further metabolized via DPH or transported via multidrug resistance-associated protein 4 (MRP4) are illustrated in **Figure 1b**.

Cellular endogenous uracil synthesis was simulated with a constant rate for each intracellular compartment, which was optimized to fit the observed data of endogenous plasma concentrations measured throughout the day. For DPD- and DPH-mediated metabolism, Michaelis–Menten kinetics were assumed, with the Michaelis–Menten constants derived from literature<sup>26,27</sup> and respective activity rates optimized to fit the observed data. Diurnal rhythms were implemented for DPD and DPH-mediated metabolism according to Eq. 1. Additionally, active transport of 5-FU and uracil via MRP4 was implemented and optimized as well. The respective drug-dependent parameters of the models are summarized in **Tables S2.2**, **S2.3**, **S3.2**, **S3.3**, and **S4.2**.

The model predictions of observed plasma concentrations of uracil as [2-<sup>13</sup>C]uracil from oral solutions, 5-FU from intravenous bolus and continuous administrations, and their metabolites are shown in selected profiles in **Figure 2**. Diurnal variations in DPD activity were implemented with  $\text{Amp}_{\text{DPD}}$  (0.124) derived from literature<sup>7</sup> and  $T_{\text{Acr,DPD}}$  optimized to fit the observed plasma concentrations. The impact of diurnal variation in DPD activity is further detailed in **Figure 3** with exemplary plasma concentration–time profiles of endogenous uracil, DHU and their corresponding parent-metabolite plasma ratio (DHU/U; often used to assess DPD phenotypes), as well as profiles of 5-FU and DHFU during continuous infusions of 5-FU with constant and chronomodulated rates.

For all model simulations presented in **Figure 3**, a literature value for  $\text{Amp}_{\text{DPD}}$  (0.124)<sup>7</sup> was used, appropriate to capture the extent of diurnal variations in mean uracil and 5-FU plasma concentrations, whereas  $T_{\text{Acr,DPD}}$  was optimized individually. Because both the constant rate infusion (**Figure 3b**) and the chronomodulated infusion (**Figure 3c**) were administered in the same cohort,<sup>36</sup>  $T_{\text{Acr,DPD}}$  of 1,285 min resulting in an acrophase at 7 PM was used for both simulations. To simulate chronomodulated infusions (**Figure 3c,d**), variations in administration rates described with the parameters Amp and  $T_{\text{Acr}}$  (here  $\text{Amp}_{\text{INF}}$  and  $T_{\text{Acr,INF}}$ ) according to Eq. 1 were estimated based on the observed plasma concentration–time profiles. Overall, patients received ~60% of the daily 5-FU dose during the night with a peak delivery rate at 4 AM.

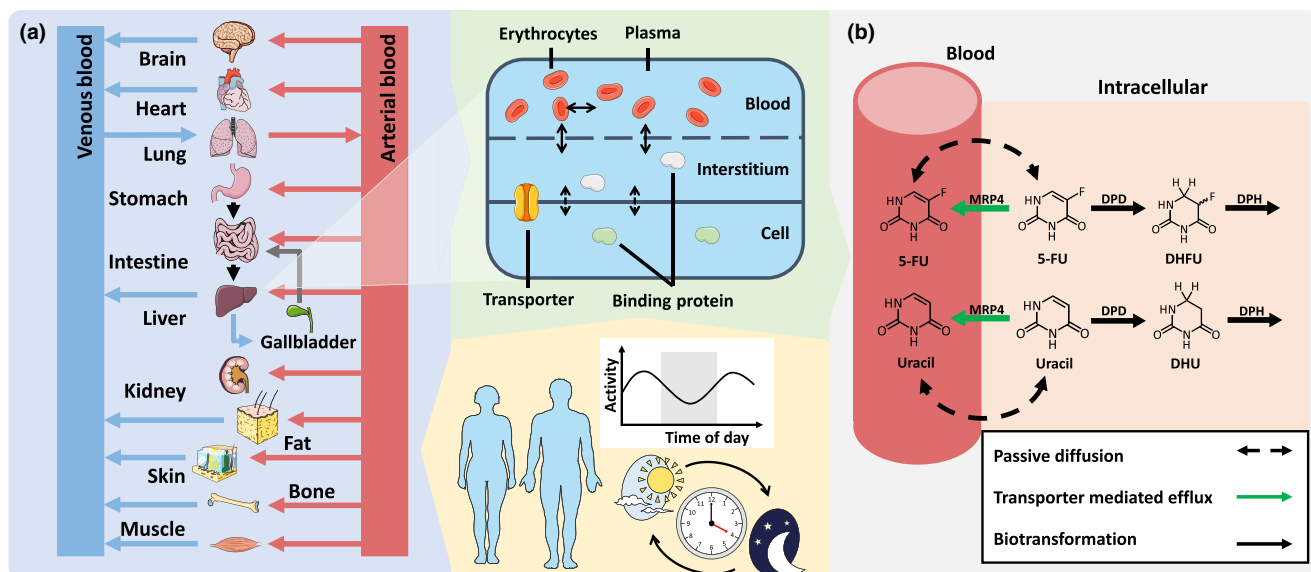


**Figure 1** Schematic overview of the PBPK models of 5-FU and uracil. (a) The whole-body PBPK model comprises compartments representing organs and tissues, interconnected via blood flow. Each organ compartment is further divided into four subcompartments: plasma, red blood cells, and interstitial and intracellular space. Multi-compartment models were built to describe and predict the PKs of 5-FU and uracil considering drug-clock time interactions. (b) An illustrative depiction of the implemented processes: 5-FU is inactivated by DPD to DHFU. DHFU is subsequently metabolized by DPH with subsequent metabolism of DHU via DPH. Drawings by Servier, licensed under CC BY 3.0.<sup>25</sup> 5-FU, 5-fluorouracil; DHFU, dihydrofluorouracil; DHU, dihydrouracil; DHP, dihydroprymidinase; DPD, dihydropyrimidine dehydrogenase; DPH, dihydropyrimidinase; DHU, dihydrouracil; MRP4, multidrug resistance-associated protein 4; PBPK, physiologically-based pharmacokinetic; U, uracil.

Additionally, diurnal variations in DPH activity were simulated based on the assumption that clock genes may influence DPH as well. The diurnal parameters for DPH activity ( $Amp_{DPH}$  and  $T_{Acr,DPH}$ ) were optimized to match the respective metabolite profiles (Figure 3a,b). By considering diurnal DPH activity, the diurnal patterns observed in the metabolite plasma concentrations were well-predicted, particularly in the case of DHFU, whose plasma levels substantially exceeded the oscillation of the parent plasma levels. MRD values for the metabolite predictions with a diurnal DPH activity were 1.06 and 1.68 for DHU and DHFU, respectively. Predictions of metabolite plasma concentrations with a constant DPH activity are shown in Sections S2.3 and S4.4.

Overall, the assessed performance of the models predicting observed plasma concentrations of 5-FU and uracil as well as their metabolites are shown in goodness-of-fit plots with selected plasma concentration-time profiles in Sections S2.4.3, S3.4.3, and S4.5.3. All predictions were in good agreement with the observed data, with 96 of 98 of predicted  $AUC_{last}$  and 27 of 28 of predicted  $C_{max}$  values within the 2-fold acceptance limits. Total GMFEs for the 5-FU and uracil model performance were 1.23 and 1.12 (1.00–2.43) for  $AUC_{last}$  values as well as 1.20 and 1.20 (1.00–2.06) for  $C_{max}$  values, respectively.

All predicted compared with observed plasma concentration-time profiles on a linear and semilogarithmic scale, as well as  $AUC_{last}$  and  $C_{max}$  values for the test and training data sets are given in Sections S2.4, S3.4, and S4.5, and MRD, MSA, and GMFE values summarized in Tables S2.4, S2.5, S3.4, S3.5, S4.3, and S4.4.

### PBPK model adaptation: Personalized dosing based on individual DPD chronotypes

To investigate the extent of IIV in DPD activity and its impact on 5-FU therapy, individual DPD chronotypes were estimated for patients with cancer and healthy subjects. DPD chronotypes in patients with cancer were derived from two different groups. First, individual DPD chronotypes were estimated from observed 5-FU plasma concentration-time profiles reported by Lévi *et al.*<sup>19</sup> (Lévi group) by adapting  $Amp_{DPD}$  and  $T_{Acr,DPD}$  to match the observed 5-FU plasma profiles for every individual (Figure 4a). Here, all 10 patients received chronomodulated 5-FU with a peak delivery rate at 4 AM. The administration rates were obtained from the respective study. Individual 5-FU plasma levels were observed to vary greatly, with peak concentrations differing by up to 12-fold between patients, despite receiving the same dose and infusion rate. Second, DPD chronotypes were extrapolated from *DPYD* mRNA expression profiles reported from cancer patients by Raida *et al.*<sup>8</sup> (Raida group). Here, the parameters  $Amp_{DPD}$  and  $T_{Acr,DPD}$  were estimated from leukocyte *DPYD* mRNA expressions, neglecting the short translation time of 1.7 minutes (translation rate of 10 amino acids per seconds<sup>38</sup> for a 1,025 amino acid long DPD protein<sup>39</sup>).

The respective values for  $Amp_{DPD}$  and  $T_{Acr,DPD}$  for the Lévi and Raida groups were used according to (Eq. 1) to calculate DPD activity over time, based on  $V_{DPD}$  (baseline DPD activity) as shown in Figure 4b,c.

DPD chronotypes in healthy individuals were determined from measured DPD enzyme activities<sup>7</sup> (Figure 4e). In healthy subjects, acrophase and extent of enzyme activity exhibited greater

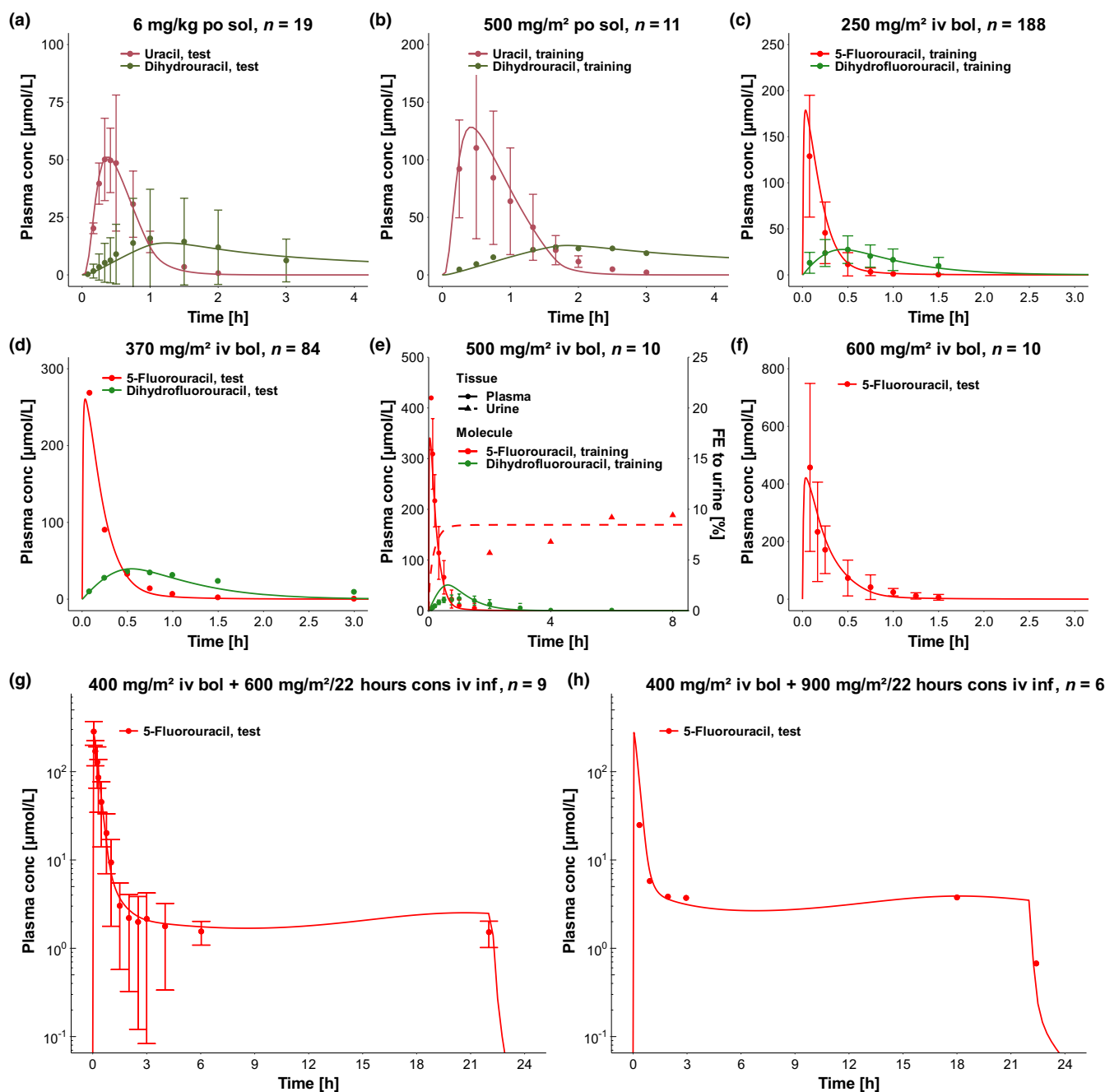


**Figure 2** PBPK model performance. (a,b) Predicted (solid lines) and observed (dots) plasma concentration-time profiles of  $[2-^{13}\text{C}]$ uracil and dihydrouracil after application of  $6\text{ mg/kg}$  body weight and  $500\text{ mg/m}^2$  body surface area  $[2-^{13}\text{C}]$ uracil as an oral solution with observed data from Mattison *et al.*<sup>28</sup> and Van Staveren *et al.*<sup>29</sup> (c–f) Predicted (solid lines) and observed (dots) plasma concentration-time profiles of 5-FU and dihydrofluorouracil after intravenous bolus injections of  $250\text{ mg/m}^2$ ,  $370\text{ mg/m}^2$ ,  $500\text{ mg/m}^2$  and  $600\text{ mg/m}^2$  5-FU with observed data from Bocci *et al.*,<sup>30</sup> Paolo *et al.*,<sup>31</sup> and Bardakji *et al.*<sup>32</sup> Additionally predicted (dashed line) and observed (triangles) fractions excreted in urine after administration of  $500\text{ mg/m}^2$  5-FU as bolus injections.<sup>33</sup> (g,h) Predicted (solid lines) and observed (dots) plasma concentration-time profiles of 5-FU after intravenous bolus injections of  $400\text{ mg/m}^2$  as loading dose and intravenous continuous infusions at a constant rate of  $600$  and  $900\text{ mg/m}^2$  over 22 hours as maintenance dose with observed data from Joel *et al.*<sup>34</sup> and Joulia *et al.*<sup>35</sup> 5-FU, 5-fluorouracil; bol, bolus injection; conc, concentration; cons, constant rate continuous infusion; inf, infusion; iv, intravenous; n, number of subjects; PBPK, physiologically-based pharmacokinetic; po, oral; sol, solution.

homogeneity, whereas both cancer patient groups displayed more pronounced IIV. This distinction is further emphasized when comparing the individual DPD maximum activity at their acrophases between healthy subjects and patients with cancer throughout the day (Figure 4d). DPD acrophases in healthy subjects were observed

during the night between 1 and 5 AM, whereas in both patients with cancer groups they were distributed across the entire day, with the majority occurring during daytime hours. The standard deviation of mean DPD acrophases for patients with cancer was 3.6-fold higher than for the healthy group ( $9:53\text{ AM} \pm 5.29$  hours for patients with

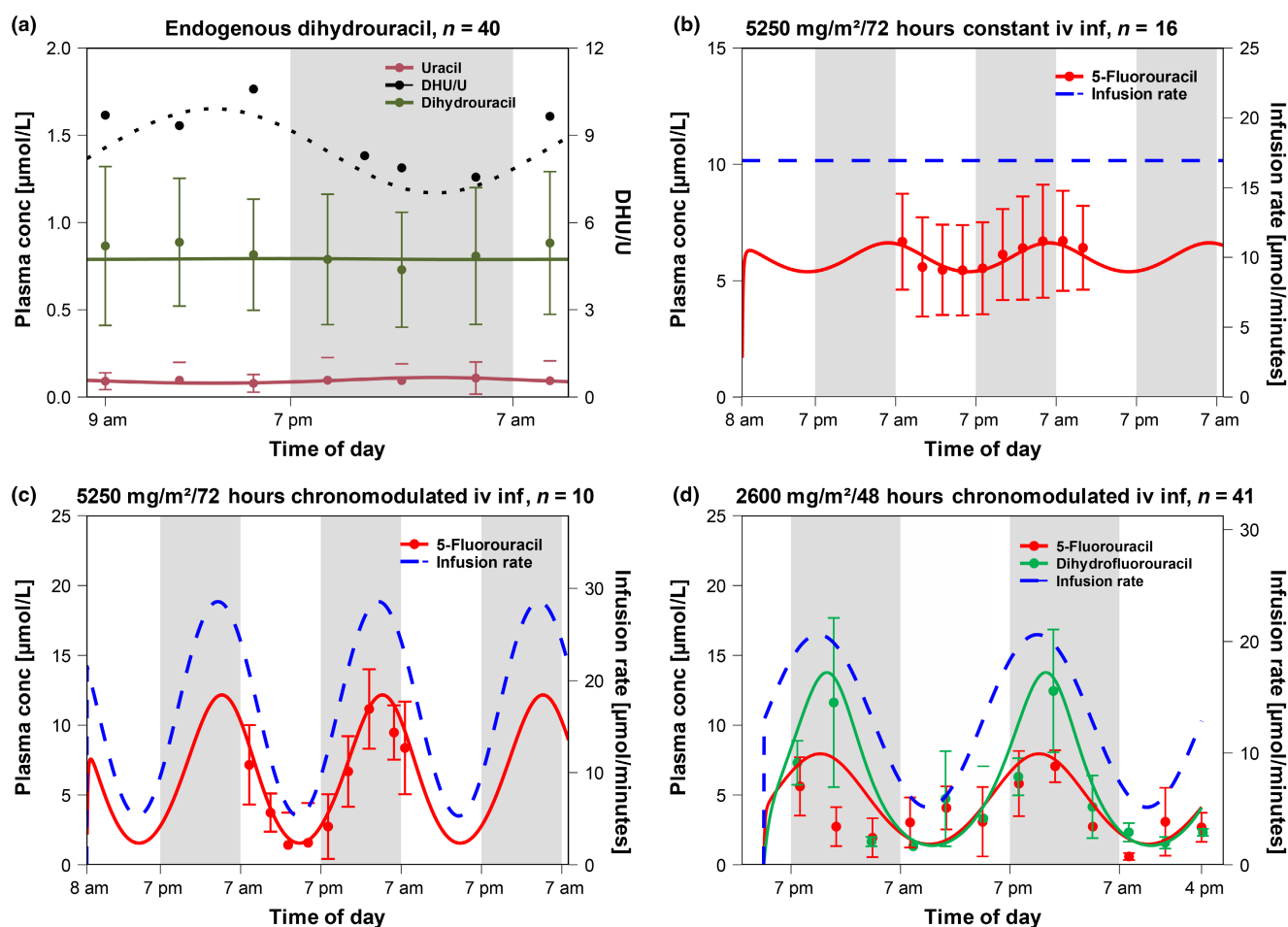


**Figure 3** Physiologically-based chronopharmacokinetic model performance. (a) Predicted (lines) and observed mean (dots) plasma concentration-time profile of endogenous uracil (U, dark red) and dihydrouracil (DHU, dark green) with respective DHU/U ratios (black).<sup>7</sup> (b) Predicted (solid line) and observed (dots) mean 5-FU plasma concentration-time profile after a constant rate infusion of 5,250 mg/m<sup>2</sup> 5-FU over 3 days (dashed line).<sup>36</sup> (c) Predicted (solid line) and observed (dots) mean 5-FU plasma concentration-time profile after a chronomodulated infusion of 5,250 mg/m<sup>2</sup> 5-FU over 3 days (dashed line).<sup>36</sup> (d) Predicted (solid lines) and observed (dots) mean 5-FU and dihydrofluorouracil plasma concentration-time profiles after a chronomodulated infusion of 2,600 mg/m<sup>2</sup> 5-FU over 48 hours (dashed line).<sup>37</sup> Dihydrouracil and dihydrofluorouracil were simulated with a DPH-mediated metabolism with an adapted diurnal activity rate. Parameters describing circadian DPD activity were derived from reported activity measurements in peripheral blood mononuclear cells (PBMCs).<sup>7</sup> 5-FU, 5-fluorouracil; conc, concentration; DHU/U, dihydrouracil to uracil plasma ratio; inf, infusion; iv, intravenous; n, number of subjects; PBMC, peripheral blood mononuclear cells; PBPK, physiologically-based pharmacokinetic.

cancer vs. 2:49 AM  $\pm$  1.45 hours for healthy subjects). The estimated maximum DPD enzyme activity for both patients with cancer and healthy subjects was more uniformly distributed in the range of 10 and 20 nmol/mg/hour (12.94  $\pm$  1.89 nmol/mg/hour for healthy subjects vs. 12.50  $\pm$  2.13 nmol/mg/hour for patients with cancer).

Overall, the importance of diurnal variations and their impact on individual plasma concentrations led to the development of a potential model-informed precision dosing approach for chronomodulated 5-FU treatment, as illustrated in Figure 5 based on 3 representative individuals from the Raida group (shown in Figure 4c). Individual DPD chronotype estimation can be performed using measured *DPYD* mRNA expressions, DPD enzyme activities (e.g., in PBMC cells) or DPD substrate concentrations, such as endogenous uracil or 5-FU plasma levels. After estimating the amplitude and acrophase ( $Amp_{DPD}$  and  $T_{Acro,DPD}$ ) required to describe diurnal DPD activity, the PBPK models were used to introduce alternative modified infusion rates for different chronomodulated infusion

scenarios. As demonstrated in Figure 5, these include (i) a chronomodulated infusion rate with peak delivery at 4 AM, resulting in comparable peak plasma concentrations, (ii) a chronomodulated infusion rate with peak rate at an individual time, resulting in comparable shapes, peak plasma concentrations and AUCs, and finally (iii) a “noise canceling” infusion rate, resulting in constant linear plasma levels.

## DISCUSSION

5-FU is a widely used and potent anticancer agent with complex PKs, which were captured and assessed by our developed PBPK models, providing a ground for further examination. In this study, both 5-FU and uracil, as well as their metabolites DHFU and DHU, were simulated to comprehensively characterize the impact of diurnal variations and their (interpatient) variability in DPD activity on drug exposure. The models are capable of predicting various administrations of intravenous and oral 5-FU across a

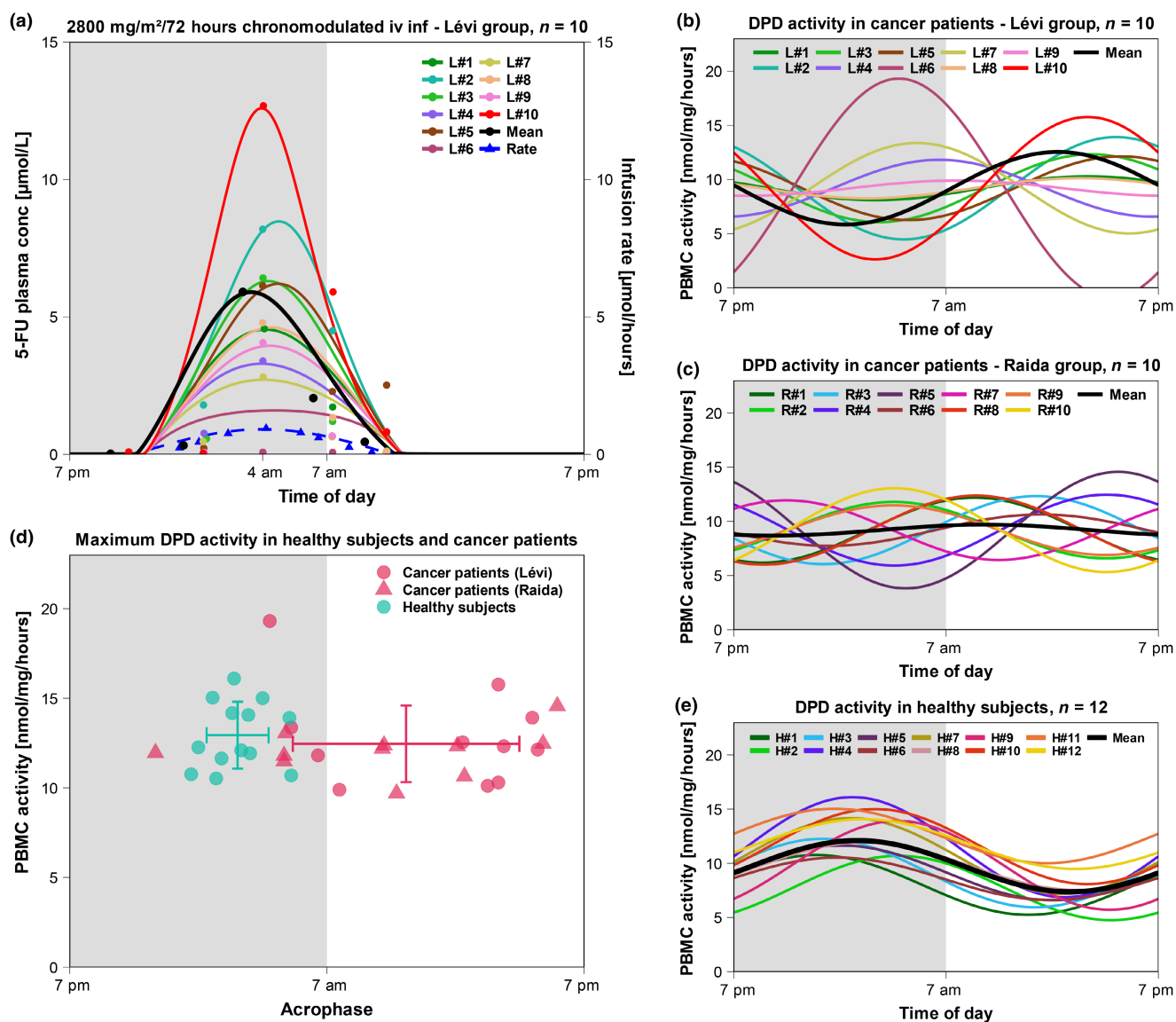


**Figure 4** IIV of DPD chronotypes in healthy subjects and patients with cancer. (a) Predicted (solid lines) and observed (dots) mean and individual 5-FU plasma concentration-time profiles after a chronomodulated hepatic arterial infusion of 2,800 mg/m<sup>2</sup> over 3 days.<sup>19</sup> The corresponding administration rate (dashed line) was simulated to fit the reported (triangles) administration rate. (b) Mean and individual DPD chronotypes in patients with cancer estimated from observed 5-FU plasma concentration-time profiles reported by Lévi *et al.*<sup>19</sup> (Lévi group). Individual DPD enzyme activities were adapted to fit the observed plasma concentration-time profiles and are shown in (a). (c) Mean and individual DPD chronotypes in cancer patients estimated from observed relative *DPYD* mRNA expression reported Raida *et al.*<sup>8</sup> (Raida group). (d) Maximum DPD activity at its respective acrophase estimated in cancer patients derived from Lévi *et al.*<sup>19</sup> and Raida *et al.*<sup>8</sup> compared with healthy subjects compiled from Jacobs *et al.*<sup>7</sup> The lines indicate mean ± SD of maximum activity and acrophase. (e) Mean and individual DPD chronotypes as enzyme activities estimated from observed DPD activities in healthy subjects reported by Jacobs *et al.*<sup>7</sup> 5-FU, 5-fluorouracil; chrono, chronomodulated; conc, concentration; DPD, dihydropyrimidine dehydrogenase; H#, healthy individual; inf, infusion; iv, intravenous; L#, patient with cancer from the Lévi group; *n*, number of individuals; PBMC, peripheral blood mononuclear cells; R#, patient with cancer from the Raida group.

broad dosing range (143–2,800 mg/m<sup>2</sup>), as well as orally administered and endogenous uracil and were successfully evaluated by comparing predicted and observed plasma concentration-time profiles and fractions excreted in urine, AUC<sub>last</sub> and C<sub>max</sub> values and calculations of their respective MRDs, MSAs, and GMFEs.

Several PK models have previously been published to describe the PK of 5-FU or uracil. For example, one approach focused on predictions of 5-FU as a metabolite of capecitabine,<sup>40</sup> whereas also describing 2 intermediate metabolites. Additionally, a PBPK model was

developed to describe the 3-step metabolism for orally administered [2-<sup>13</sup>C]uracil.<sup>41</sup> A previously published semimechanistic PK model, which assessed interpatient variability for PK parameters, modeled chronomodulated infusions of 5-FU with irinotecan and oxaliplatin.<sup>18</sup> Our study builds on the concepts of these previously published models and incorporates a broad dosing range for various administrations, including constant and chronomodulated infusions of 5-FU, endogenous synthesis of uracil, and diurnal variations in DPD and DPH activity, as well as 5-FU and uracil metabolites. Moreover, our

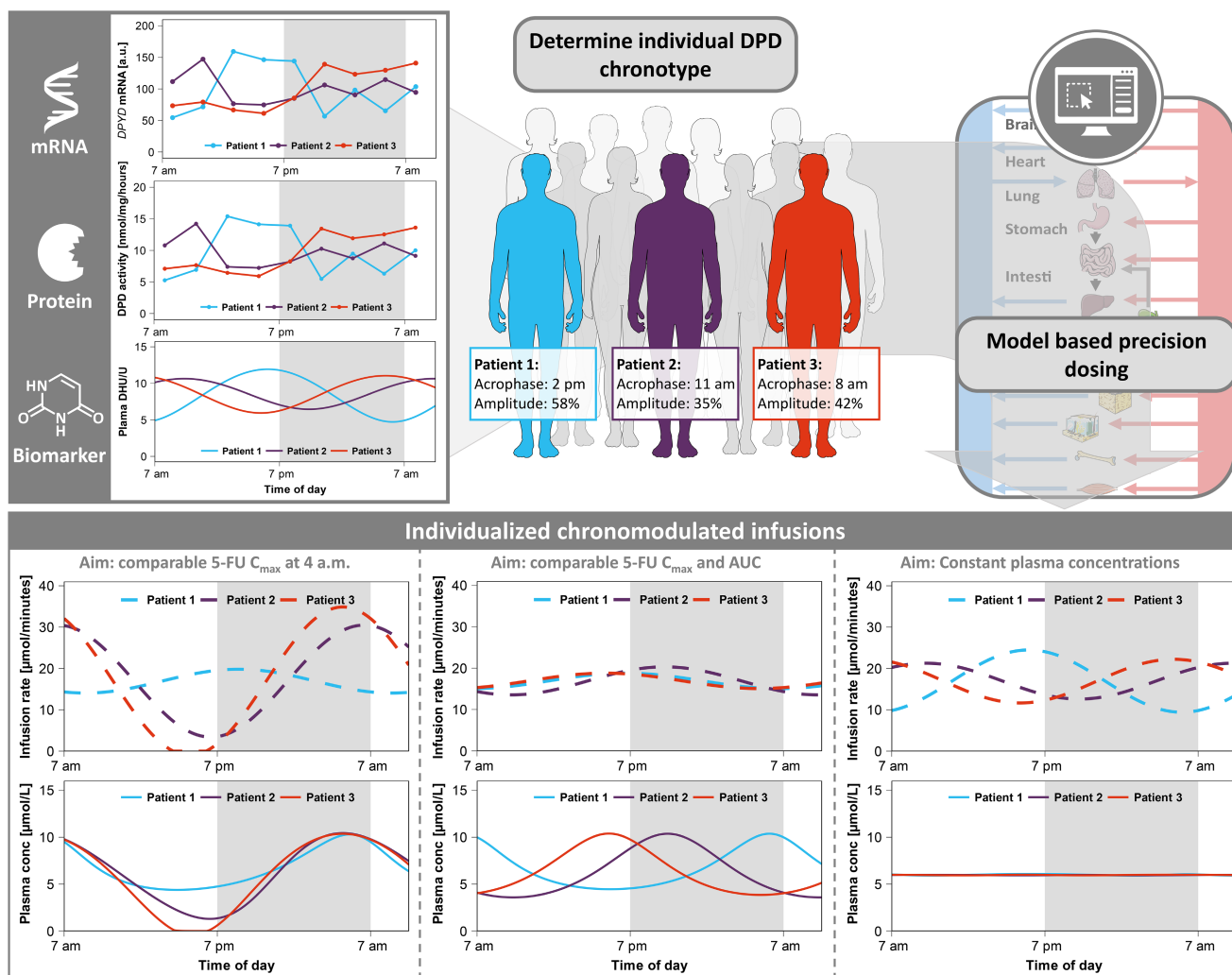


**Figure 5** Model-based chronomodulated precision dosing. To address the prevalent interindividual variability in diurnal variations concerning 5-FU treatment, a model-based precision dosing approach was developed using the presented PBPK models. The DPD chronotype can be determined through measurements of *DPYD* mRNA expressions, DPD enzyme activities, or endogenous plasma levels of dihydrouracil and uracil. Upon estimating the  $T_{Ac}$  and  $Amp_{DPD}$  (in this example, for 3 individuals), the respective parameters can be utilized to simulate diurnal DPD activities according to Eq. 1. Here, 3 scenarios were simulated: individual chronomodulated infusion of 5,250 mg/m<sup>2</sup> 5-FU over 3 days with (left) individual peak rates at 4 AM to achieve similar  $C_{max}$  at 4 AM; (middle) individual peak rates at individual clock times to achieve similar  $C_{max}$  and AUC with a similar shape in the plasma concentration–time profiles; (right) “noise canceling” infusion rates to achieve constant plasma concentrations. The infusion rates are illustrated in the top row (dashed lines) and the respective 5-FU plasma concentrations are shown in the bottom row (solid lines). 5-FU, 5-fluorouracil; a.u., arbitrary units; AUC, area under plasma concentration–time curve;  $C_{max}$ , maximum plasma concentration; conc, concentration; DPD, dihydropyrimidine dehydrogenase; *DPYD*, gene coding for dihydropyrimidine dehydrogenase; DHU/U: dihydrouracil to uracil plasma ratio, mRNA: messenger ribonucleic acid; PBPK, physiologically-based pharmacokinetic.

models incorporate an efflux transporter mimicking MRP4's active transport,<sup>42</sup> as both 5-FU and uracil are subject to a variety of transporter proteins,<sup>43–46</sup> of which MRP4 and its associated *ABCC4* gene polymorphisms were discussed to impact on treatment efficacy for colorectal cancer in 5-FU and capecitabine chemotherapy.<sup>24</sup>

As fluctuating plasma levels were observed in literature,<sup>7,37</sup> diurnal variations in DPD activity were effectively incorporated using a time-dependent sine function. Additionally, diurnal activity in DPH was simulated, based on the assumption that human cellular clocks influence DPH, similarly to observed diurnal patterns in DPH activity in mice.<sup>47</sup> In the case of endogenous uracil, differences in the oscillation of metabolite plasma levels between the simulated constant and circadian DPH activities were negligible,

although these data were measured in healthy subjects.<sup>7</sup> In patients with cancer, oscillations in plasma concentrations were more pronounced for DHFU than for 5-FU, the parent, itself.<sup>37</sup> Here, the metabolite plasma levels were successfully predicted only when assuming diurnal variations to impact DPH as well. However, it remains unclear if and to what extent DPH is under circadian control and whether differences in diurnal activity exist between healthy subjects and patients with cancer, or between endogenous uracil and administered 5-FU.

Nonetheless, the impact on DPH activity may be of relevance, for instance, when using endogenous uracil or DHU/U ratios as biomarkers for DPD activity. Before initiating treatment with fluoropyrimidine-based medications, it is suggested to undertake



alternative or complementary testing for DPD phenotyping in addition to *DPYD* genotyping. These recommendations are in accordance with the guidelines proposed by the European Medicines Agency and various international guidelines.<sup>4,48</sup> Phenotyping methods often include single measurements of DHU/U ratios.<sup>4,48</sup> Regardless of the phenotyping method, such as DHU/U plasma or DPD PBMC activity measurements, clinicians should generally consider conducting repeated measurements over 24 hours when phenotyping for DPD. This would enable a more accurate prediction of its activity in polymorphic patients and consequently improve efficacy and safety in fluoropyrimidine treatment.

Within the framework of 5-FU treatment, simulations were conducted to model diurnal variations for both average and individual DPD chronotypes. For the underlying DPD chronotypes of observed mean plasma concentrations in study populations,  $Amp_{DPD}$  could be described by two values derived from literature (0.124<sup>9</sup> and 0.245<sup>7</sup>), whereas  $T_{Acr}$  differed for most study populations and had to be estimated for each profile.<sup>7,9</sup> When simulating plasma concentrations for individual patients, parameters  $Amp_{DPD}$  and  $T_{Acr}$  had to be adapted individually, as patients showed pronounced IIV in their DPD chronotypes.

In general, DPD chronotypes could be estimated (i) retrospectively from observed DPD substrate concentrations, such as 5-FU plasma concentrations, (ii) from observed DPD enzyme activities, or (iii) from observed *DPYD* mRNA expressions in leukocytes. Although, whereas DPD activity perfectly correlates with 5-FU clearance,<sup>20</sup> knowledge on the correlation between 5-FU clearance and *DPYD* mRNA expression is missing. In this analysis, the correlation between 5-FU clearance and *DPYD* mRNA expression was explored, acknowledging the challenges in establishing a direct relationship. Although a calculated very short translation rate (1.7 minutes) was used to extrapolate DPD enzyme activity from *DPYD* mRNA expression, the timing and extent of this correlation, particularly considering the enzyme's activity, require further investigation, as studies such as Barrat *et al.*,<sup>49</sup> which observed circadian variations in DPD activity in specific tissues (e.g., oral mucosa, suggested that this relationship might be complex and tissue-dependent). Understanding these nuances is essential before confidently using such correlations to chronotype patients for DPD in a clinical setting.

Lévi *et al.*<sup>19</sup> treated patients with 5-FU via a hepatic artery infusion with a peak rate at 4 AM. Although individual plasma concentrations showed a consistent time to reach  $C_{max}$  ( $T_{max}$ ) due to uniform drug administration rates, there was still significant variability between individuals in  $C_{max}$  with an up to a 12-fold difference between minimum and maximum observed  $C_{max}$  values. Similarly, interpatient variability was apparent among individual DPD chronotypes extrapolated from the patients' 5-FU plasma concentration-time profiles, particularly concerning their respective acrophases, which is comparable to IIV estimated from DPD chronotypes extrapolated from *DPYD* mRNA expressions measured in patients with cancer. A lower IIV was observed in DPD activities measured in healthy volunteers.<sup>8</sup> When comparing estimated DPD chronotypes in healthy subjects and patients with cancer, acrophases were homogenous within nighttime for healthy individuals. In contrast, acrophases for the patients with cancer groups were distributed throughout the day. Although the

presented modeling approach successfully captured IIV in diurnal DPD function, inherent limitations may exist in estimating diurnal parameters ( $Amp$  and  $T_{Acr}$ ) from sparse PK data. Future studies with more extensive data sets are required to validate and refine these estimations, ensuring a more robust understanding of the circadian rhythm of DPD function in patients with cancer. However, recent advances in circadian biology introduce methods to determine an individual's circadian phase without frequent biosamples. These techniques use biomolecular markers and computational analyses, offering a less invasive patient chronotyping.<sup>50</sup> Although, extension of these established methods to assess the DPD chronotype would have to be investigated further.

The notable IIV in DPD chronotypes among patients with cancer suggests that a uniform chronomodulated infusion rate could result in varying efficacy. For instance, Takimoto *et al.*<sup>51</sup> reported no major differences in toxicity for 5-FU therapy between constant and chronomodulated infusions. Conversely, in a phase III trial comparing conventional to chronomodulated chemotherapy conducted in 2006, the treatment efficacy of infusional 5-FU administered with a constant rate and a chronomodulated rate was investigated.<sup>16</sup> Here, an increase in response rates and overall survival as well as a decrease in grade 3–4 toxicities was observed in men receiving chronomodulated cancer therapy. However, women experienced lower response rates and overall survival along with increased toxicities.<sup>16</sup> In case of chronomodulated therapy with other anticancer drugs, irinotecan is widely discussed regarding differences in tolerability between men and women.<sup>52</sup> One approach for personalizing chronomodulated irinotecan treatment was based on the patient's sex. Here, Innominato *et al.* investigated the time of lowest toxicity of irinotecan, finding that men tolerated irinotecan better when receiving peak delivery in the morning, whereas women experienced the least toxicity in the afternoon.<sup>52</sup> In this case, patients would benefit from receiving irinotecan treatment tailored to their respective sex. Similarly, this could suggest a potential advantage of personalized dosing for anticancer treatment with 5-FU.

To offer an alternative to chronomodulated 5-FU infusions with uniformed peak rate at 4 AM, different scenarios were simulated in virtual individuals exhibiting estimated DPD activities from the Raida cancer patient group.<sup>8</sup> Instead of a common peak rate at 4 AM, infusion rates were simulated to achieve comparable peak concentrations at 4 AM. Additionally, infusion rates were adapted to reach comparable 5-FU peak concentrations at individual clock times to maintain comparable shapes in their plasma concentration-time curves. We accomplished this by adjusting the peak rate during periods of minimum DPD enzyme activity to prevent excessively high infusion rates. Additionally, we tested an individualized “noise-canceling” infusion rate to maintain constant plasma levels of 5-FU.

The clinical impact of achieving peak 5-FU plasma levels at different clock times compared with 4 AM on therapy efficacy and tolerability for individual patients remains to be determined in dedicated studies specifically designed to examine personalized chronomodulated 5-FU treatment. Relevant chronopharmacodynamic pathways which involve the formation of intracellular active metabolites or target enzyme activity, such as thymidylate synthase, were not implemented, as relevant data were unavailable. These factors deserve further investigation and consideration in future adaptations of 5-FU treatment strategies. Moreover, several assumptions

had to be made for model development and its application for personalized chronomodulated treatment simulations. This might lead to potential sources of bias as well as related limitations and risks including (i) missing data from clinical study reports on time of administration and thus description of related diurnal DPD parameters, (ii) on demographic data mainly body surface area leading to potentially inadequately estimated simulated dosing, (iii) inclusion criteria of the clinical trials resulting in heterogeneous distributions in the study demographics and the respective physiology, and (iv) pathophysiology and co-administration of the included patients, as well as (v) the pharmacological implications of the chronopharmacodynamic processes of 5-FU treatment. Nonetheless, the presented PBPK models might be useful to guide the design of dosing adaptation by simulating various 5-FU treatment scenarios based on individual DPD chronotypes.

In summary, the developed whole-body PBPK models effectively describe and predict the complexity of 5-FU PKs, as they account for the significant interpatient variability in DPD chronotypes and their impact on 5-FU therapy. The developed models might be particularly impactful for the future practice of cancer medicine as they provide an innovative framework for precision dosing of 5-FU based on patients' unique DPD chronotypes. The Open Systems Pharmacology (OSP) framework was utilized for a detailed mechanistic implementation of 5-FU PKs inside a whole-body PBPK framework and, thus, the flexibility to address 5-FU chronopharmacology at both organ and cellular levels. In contrast, Bayesian frameworks in population PK approaches might be superior capturing IIV but require specific individual data sets and typically lack mechanistic depth. Future advancements may pave the way for more integrative modeling methods that could improve our mechanistic understanding on a patient-individual level. For this, the developed PBPK models are publicly available for open access (GitHub repository on <http://models.clinicalpharmacy.me>). [Correction added on 31 January 2024, after first online publication: In the above sentence, URL to GitHub repository has been corrected in this version.] However, they could guide design and dosage adaptations in future clinical trials, emphasizing their translational relevance in the field of oncology.

#### SUPPORTING INFORMATION

Supplementary information accompanies this paper on the *Clinical Pharmacology & Therapeutics* website ([www.cpt-journal.com](http://www.cpt-journal.com)).

#### FUNDING

R.D.'s work is supported by a grant from Cancer Research UK (C53720/A29468) and Anglo American Platinum. J.J.S., H.J.G., and M.S. were supported by the European Commission Horizon 2020 UPGx grant 668353. Moreover, M.S. was funded by the Robert Bosch Stiftung (Stuttgart, Germany), a grant from the German Federal Ministry of Education and Research (BMBF 031L0188D), and the Deutsche Forschungsgemeinschaft (DFG, German Research Foundation) under Germany's Excellence Strategy—EXC 2180—390900677. T.L. was supported by the project “Open-source modeling framework for automated quality control and management of complex life science system models” (OSMOSES) funded by the German Federal Ministry of Education and Research (BMBF, grant ID:031L0161C).

#### CONFLICTS OF INTEREST

Since January 2020, J.-G.W. is an employee of Boehringer Ingelheim Pharma GmbH and Co. KG. All other authors declared no competing interests for this work.

#### AUTHOR CONTRIBUTIONS

All authors wrote the manuscript and designed the research. F.Z.M. performed the research. F.Z.M. and D.S. analyzed the data.

#### ACKNOWLEDGMENT

Open Access funding enabled and organized by Projekt DEAL.

© 2024 The Authors. *Clinical Pharmacology & Therapeutics* published by Wiley Periodicals LLC on behalf of American Society for Clinical Pharmacology and Therapeutics.

This is an open access article under the terms of the [Creative Commons Attribution-NonCommercial](https://creativecommons.org/licenses/by-nc/4.0/) License, which permits use, distribution and reproduction in any medium, provided the original work is properly cited and is not used for commercial purposes.

- Sara, J.D. et al. 5-fluorouracil and cardiotoxicity: a review. *Ther. Adv. Med. Oncol.* **10**, 175883591878014 (2018).
- Diasio, R.B. & Harris, B.E. Clinical pharmacology of 5-fluorouracil. *Clin. Pharmacokinet.* **16**, 215–237 (1989).
- Meta-Analysis Group In Cancer et al. Toxicity of fluorouracil in patients with advanced colorectal cancer: effect of administration schedule and prognostic factors. *J. Clin. Oncol.* **16**, 3537–3541 (1998).
- Amstutz, U. et al. Clinical pharmacogenetics implementation consortium (CPIC) guideline for Dihydropyrimidine dehydrogenase genotype and fluoropyrimidine dosing: 2017 update. *Clin. Pharmacol. Ther.* **103**, 210–216 (2017).
- Deenen, M.J. et al. Upfront genotyping of DPYD\*2A to individualize fluoropyrimidine therapy: a safety and cost analysis. *J. Clin. Oncol.* **34**, 227–234 (2016).
- Mormont, M.C. & Levi, F. Cancer chronotherapy: principles, applications, and perspectives. *Cancer* **97**, 155–169 (2003).
- Jacobs, B.A.W. et al. Pronounced between-subject and circadian variability in thymidylate synthase and dihydropyrimidine dehydrogenase enzyme activity in human volunteers. *Br. J. Clin. Pharmacol.* **82**, 706–716 (2016).
- Raida, M. et al. Circadian variation of dihydropyrimidine dehydrogenase mRNA expression in leukocytes and serum cortisol levels in patients with advanced gastrointestinal carcinomas compared to healthy controls. *J. Cancer Res. Clin. Oncol.* **128**, 96–102 (2002).
- Jiang, H., Lu, J. & Ji, J. Circadian rhythm of dihydropyrimidine/uracil ratios in biological fluids: a potential biomarker for dihydropyrimidine dehydrogenase levels. *Br. J. Pharmacol.* **141**, 616–623 (2004).
- Harris, B., Song, R., Soong, S.-J. & Diasio, R. Relationship between dihydropyrimidine dehydrogenase activity and plasma 5-fluorouracil levels with evidence for circadian variation of enzyme activity and plasma. *Cancer Res.* **50**, 197–201 (1990).
- Metzger, G. et al. Spontaneous or imposed circadian changes in plasma concentrations of 5-fluorouracil coadministered with folinic acid and oxaliplatin: relationship with mucosal toxicity in patients with cancer. *Clin. Pharmacol. Ther.* **56**, 190–201 (1994).
- Lévi, F., Giacchetti, S., Adam, R., Zidani, R., Metzger, G. & Misset, J.L. Chronomodulation of chemotherapy against metastatic colorectal cancer. *Eur. J. Cancer* **31**, 1264–1270 (1995).
- Petit, E. et al. Circadian rhythm-varying plasma concentration of 5-fluorouracil during a five-day continuous venous infusion at a constant rate in cancer patients. *Cancer Res.* **48**, 1676–1679 (1988).
- Lévi, F., Okyar, A., Dulong, S., Innominato, P.F. & Clairambault, J. Circadian timing in cancer treatments. *Annu. Rev. Pharmacol. Toxicol.* **50**, 377–421 (2010).
- Zeng, Z.L. et al. Circadian rhythm in dihydropyrimidine dehydrogenase activity and reduced glutathione content in peripheral blood of nasopharyngeal carcinoma patients. *Chronobiol. Int.* **22**, 741–754 (2005).
- Giacchetti, S. et al. Phase III trial comparing 4-day chronomodulated therapy versus 2-day conventional delivery of fluorouracil, leucovorin, and oxaliplatin As first-line chemotherapy

- of metastatic colorectal cancer: the European organisation for research and treatment of can. *J. Clin. Oncol.* **24**, 3562–3569 (2006).
17. Giacchetti, S. *et al.* Sex moderates circadian chemotherapy effects on survival of patients with metastatic colorectal cancer: a meta-analysis. *Ann. Oncol. Off. J. Eur. Soc. Med. Oncol.* **23**, 3110–3116 (2012).
  18. Hill, R.J.W., Innominato, P.F., Lévi, F. & Ballesta, A. Optimizing circadian drug infusion schedules towards personalized cancer chronotherapy. *PLoS Comput. Biol.* **16**, e1007218 (2020).
  19. Lévi, F. *et al.* Pharmacokinetics of irinotecan, oxaliplatin and 5-fluorouracil during hepatic artery chronomodulated infusion: a translational European OPTILIV study. *Clin. Pharmacokinet.* **56**, 165–177 (2017).
  20. Fleming, R.A. *et al.* Correlation between dihydropyrimidine dehydrogenase activity in peripheral mononuclear cells and systemic clearance of fluorouracil in cancer patients. *Cancer Res.* **52**, 2899–2902 (1992).
  21. Lippert, J. *et al.* Open systems pharmacology community—an open access, open source, Open Science approach to modeling and simulation in pharmaceutical sciences. *CPT Pharmacometrics Syst. Pharmacol.* **8**, 878–882 (2019).
  22. Wojtyniak, J., Britz, H., Selzer, D., Schwab, M. & Lehr, T. Data digitizing: accurate and precise data extraction for quantitative systems pharmacology and physiologically-based pharmacokinetic modeling. *CPT Pharmacometrics Syst. Pharmacol.* **9**, 322–331 (2020).
  23. Meyer, M., Schneckener, S., Ludewig, B., Kuepfer, L. & Lippert, J. Using expression data for quantification of active processes in physiologically based pharmacokinetic modeling. *Drug Metab. Dispos.* **40**, 892–901 (2012).
  24. Chen, Q. *et al.* A polymorphism in ABCC4 is related to efficacy of 5-FU/capecitabine-based chemotherapy in colorectal cancer patients. *Sci. Rep.* **7**, 7059 (2017).
  25. Les Laboratoires Servier. Servier Medical At <<https://smart.servier.com/>> (assessed on 10 February 2022).
  26. Hishinuma, E. *et al.* Functional characterization of 21 allelic variants of dihydropyrimidinase. *Biochem. Pharmacol.* **143**, 118–128 (2017).
  27. Yamazaki, S., Hayashi, M., Toth, L.N. & Ozawa, N. Lack of interaction between propridine and 5-fluorouracil on human dihydropyrimidine dehydrogenase. *Xenobiotica* **31**, 25–31 (2001).
  28. Mattison, L.K. The uracil breath test in the assessment of dihydropyrimidine dehydrogenase activity: pharmacokinetic relationship between expired 13CO<sub>2</sub> and plasma [2-13C] dihydropyrimidine. *Clin. Cancer Res.* **12**, 549–555 (2006).
  29. Van Staveren, M.C., Theeuwes-Oonk, B., Guchelaar, H.J., Van Kuilenburg, A.B.P. & Maring, J.G. Pharmacokinetics of orally administered uracil in healthy volunteers and in DPD-deficient patients, a possible tool for screening of DPD deficiency. *Cancer Chemother. Pharmacol.* **68**, 1611–1617 (2011).
  30. Bocci, G. *et al.* A pharmacokinetic-based test to prevent severe 5-fluorouracil toxicity. *Clin. Pharmacol. Ther.* **80**, 384–395 (2006).
  31. Di Paolo, A. *et al.* Relationship between 5-fluorouracil disposition, toxicity and. *Ann. Oncol.* **12**, 1301–1306 (2001).
  32. Bardakji, Z., Jolivet, J., Langelier, Y., Besner, J.-G. & Ayoub, J. 5-Fluorouracil-metronidazole combination therapy in metastatic colorectal cancer. *Cancer Chemother. Pharmacol.* **18**, 140–144 (1986).
  33. Heggie, G.D., Sommadossi, J.P., Cross, D.S., Huster, W.J. & Diasio, R.B. Clinical pharmacokinetics of 5-fluorouracil and its metabolites in plasma, urine, and bile. *Cancer Res.* **47**, 2203–2206 (1987).
  34. Joel, S.P. *et al.* Lack of pharmacokinetic interaction between 5-fluorouracil and oxaliplatin. *Clin. Pharmacol. Ther.* **76**, 45–54 (2004).
  35. Joulia, J.M., Pinguet, F., Ychou, M., Duffour, J., Astre, C. & Bressolle, F. Plasma and salivary pharmacokinetics of 5-fluorouracil (5-FU) in patients with metastatic colorectal cancer receiving 5-FU bolus plus continuous infusion with high-dose Folinic acid. *Eur. J. Cancer* **35**, 296–301 (1999).
  36. Grem, J.L. *et al.* N-(phosphonacetyl)-l-aspartate and calcium leucovorin modulation of fluorouracil administered by constant rate and circadian pattern of infusion over 72 hours in metastatic gastrointestinal adenocarcinoma. *Ann. Oncol.* **12**, 1581–1587 (2001).
  37. Falcone, A. *et al.* 5-fluorouracil administered as a 48-hour Chronomodulated infusion in combination with leucovorin and cisplatin: a randomized phase II study in metastatic colorectal cancer. *Oncology* **61**, 28–35 (2001).
  38. Shamir, M., Bar-On, Y., Phillips, R. & Milo, R. SnapShot: timescales in cell biology. *Cell* **164**, 1302–1302.e1 (2016).
  39. Genecards entry for DPD. <<https://www.genecards.org/cgi-bin/carddisp.pl?gene=DPYD&keywords=dpd>> (accessed on 15.02.2022).
  40. Tsukamoto, Y. *et al.* A physiologically based pharmacokinetic analysis of capecitabine, a triple prodrug of 5-FU, in humans: the mechanism for tumor-selective accumulation of 5-FU. *Pharm. Res.* **18**, 1190–1202 (2001).
  41. Ito, S. *et al.* Physiologically based pharmacokinetic modelling of the three-step metabolism of pyrimidine using 13C-uracil as an in vivo probe. *Br. J. Clin. Pharmacol.* **60**, 584–593 (2005).
  42. Protein-Atlas entry for ABCC4. <<https://www.proteinatlas.org/ENSG00000125257-ABCC4/tissue>> (assessed on 10 February 2022).
  43. Mata, J.F. *et al.* Role of the human concentrative nucleoside transporter (hCNT1) in the cytotoxic action of 5[prime]-deoxy-5-fluorouridine, an active intermediate metabolite of capecitabine, a novel oral anticancer drug. *Mol. Pharmacol.* **59**, 1542–1548 (2001).
  44. Kobayashi, Y., Ohshiro, N., Sakai, R., Ohbayashi, M., Kohyama, N. & Yamamoto, T. Transport mechanism and substrate specificity of human organic anion transporter 2 (hOat2 [SLC22A7]). *J. Pharm. Pharmacol.* **57**, 573–578 (2005).
  45. Lostao, M.P., Mata, J.F., Larrayoz, I.M., Inzillo, S.M., Casado, F.J. & Pastor-Anglada, M. Electrogenic uptake of nucleosides and nucleoside-derived drugs by the human nucleoside transporter 1 (hCNT1) expressed in *Xenopus laevis* oocytes. *FEBS Lett.* **481**, 137–140 (2000).
  46. Yuan, J.-H. *et al.* Breast cancer resistance protein expression and 5-fluorouracil resistance. *Biomed. Environ. Sci.* **21**, 290–295 (2008).
  47. Zhang, R., Lahens, N.F., Ballance, H.I., Hughes, M.E. & Hogenesch, J.B. A circadian gene expression atlas in mammals: implications for biology and medicine. *Proc. Natl. Acad. Sci. U. S. A.* **111**, 16219–16224 (2014).
  48. European Medicines Agency (EMA). 5-Fluorouracil (i.v.), capecitabine and tegafur containing products: Pre-treatment testing to identify DPD-deficient patients at increased risk of severe toxicity Patients with partial or complete dihydropyrimidine dehydrogenase (DPD) deficiency ar (2020).
  49. Barrat, M.A., Renée, N., Mormont, M.C., Milano, G. & Levi, F. Étude des variations circadiennes de l'activité de la dihydropyrimidine déshydrogénase (DPD) dans la muqueuse buccale chez des sujets volontaires sains. *Pathol. Biol.* **51**, 191–193 (2003).
  50. Woelders, T. *et al.* Machine learning estimation of human body time using metabolomic profiling. *Proc. Natl. Acad. Sci.* **120**, 2017 (2023).
  51. Takimoto, C.H. *et al.* High inter- and inpatient variation in 5-fluorouracil plasma concentrations during a prolonged drug infusion. *Clin. Cancer Res.* **5**, 1347–1352 (1999).
  52. Innominato, P.F. *et al.* Sex-dependent least toxic timing of irinotecan combined with chronomodulated chemotherapy for metastatic colorectal cancer: randomized multicenter EORTC 05011 trial. *Cancer Med.* **9**, 4148–4159 (2020).